Observation of two-dimensional discrete solitons in optically induced nonlinear photonic lattices

Jason W. Fleischer*†, Mordechai Segev*†, Nikolaos K. Efremidis‡ & Demetrios N. Christodoulides‡

** Physics Department, Technion—Israel Institute of Technology, Haifa 32000, Israel*
† Electrical Engineering Department, Princeton University, New Jersey 08544, USA
‡ School of Optics/CREOL, University of Central Florida, Florida 32816-2700, USA

Nonlinear periodic lattices occur in a large variety of systems, such as biological molecules[1], nonlinear optical waveguides[2], solid-state systems[3] and Bose–Einstein condensates[4]. The underlying dynamics in these systems is dominated by the interplay between tunnelling between adjacent potential wells and nonlinearity[1–15]. A balance between these two effects can result in a self-localized state: a lattice or 'discrete' soliton[1,2]. Direct observation of lattice solitons has so far been limited to one-dimensional systems, namely in arrays of nonlinear optical waveguides[2,9–17]. However, many fundamental features are expected to occur in higher dimensions, such as vortex lattice solitons[18], bright lattice solitons that carry angular momentum, and three-dimensional collisions between lattice solitons. Here, we report the experimental observation of two-dimensional (2D) lattice solitons. We use optical induction, the interference of two or more plane waves in a photosensitive material, to create a 2D photonic lattice in which the solitons form[11,12]. Our results pave the way for the realization of a variety of nonlinear localization phenomena in photonic lattices and crystals[19–23]. Finally, our observation directly relates to the proposed lattice solitons in Bose–Einstein condensates[4], which can be observed in optically induced periodic potentials[24,25].

In general, wave propagation in periodic lattices (such as an array of optical waveguides) is fundamentally different from that occurring in a homogeneous medium. For example, when light is focused into one waveguide, linear propagation along the waveguides results in tunnelling to adjacent sites, exhibiting a characteristic diffraction pattern with the intensity mainly concentrated in the outer lobes. For a sufficiently high nonlinearity, self-focusing can balance this effect, leading to a lattice (discrete) soliton[2,9,10]. For light propagating at an angle $\theta = k_x/k \approx k_x/k_z$ with respect to the array, the periodicity of the lattice becomes important, as the corresponding 'Bloch momentum' k_x can satisfy Bragg reflection conditions within the Brillouin zone (defined in the range $|k_x D| \leq \pi$, where D is the lattice spacing). Near the edge of this zone, diffraction becomes anomalous ('negative'), leading to such effects as diffraction management[13,14] and staggered (π out-of-phase) solitons[11,15,17]. These are some of the fundamental aspects of solitons in nonlinear periodic structures, which were originally discovered through the theoretical paradigm of the discrete nonlinear Schrödinger equation[1–4,16], hence the term 'discrete soliton'[1,2]. Experimentally, self-localized 'breathers' have been observed in various physical settings[5–8], but lattice (discrete) solitons have thus far been reported only in nonlinear optical systems and only in one-dimensional (1D) configurations[9–11,13,17]. In what follows we demonstrate bright 2D lattice solitons in their simplest realization: in-phase solitons at the base of the first Brillouin zone. In addition, we demonstrate bright self-trapped wave packets at the edge of the first Brillouin zone.

The formation of the 2D nonlinear photonic lattice relies on an optical induction technique[11,12] in which a 2D array of waveguides is induced in a nonlinear medium. We proposed this method theoretically[12] and recently demonstrated experimentally[11] 1D lattice solitons in a 1D waveguide array. The waveguide array is induced, in real time, in a photosensitive material by interfering two or more plane waves. A separate 'probe' beam is launched into the periodic waveguide array, where it exhibits discrete diffraction and, at a sufficiently high nonlinearity, forms a lattice soliton. For this system to work, it is essential that the waveguides are as uniform as possible, implying that the interference pattern (inducing the lattice) must not change in the propagation direction. For this to happen in the nonlinear medium, the interfering waves themselves should not be affected by the nonlinearity. At the same time, the probe (soliton-forming) beam must experience the highest possible nonlinearity. A photorefractive material with a strong electro-optic anisotropy allows this scenario; the interfering beams are polarized in a non-electro-optic direction and the probe is polarized along the crystalline c axis. In this arrangement, the interfering beams will propagate mostly linearly, while the signal beam will experience both a periodic potential and a significant (screening) nonlinearity[26,27]. In this way we have demonstrated both on-axis and staggered 1D lattice solitons[11]. However, 1D systems, although quite instructive, cannot host a variety of fascinating nonlinear phenomena that require a higher lattice dimensionality. Our method of optical lattice induction allows for dynamic, reconfigurable arrays of almost any geometry.

This method of optical induction is quite general, allowing the

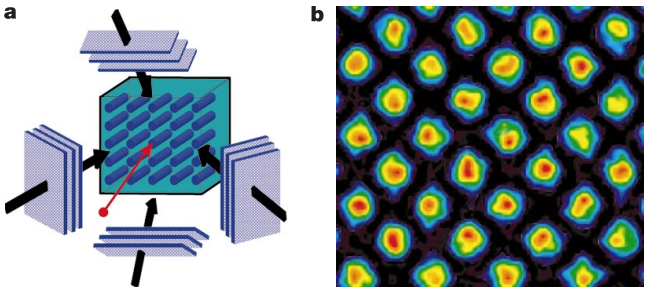

Figure 1 Experimental scheme and a typical photonic lattice. **a**, Diagram of our experimental set-up. We use a photosensitive (photorefractive) crystal with electro-optic anisotropy: two interfering pairs of ordinarily polarized plane waves induce the photonic array, while the extraordinarily polarized probe (soliton-forming) beam is focused into a single waveguide. **b**, Typical observation of a waveguide array at the exit face of the crystal. Each waveguide is approximately 7 μm in diameter, with an 11 μm spacing between nearest neighbours.

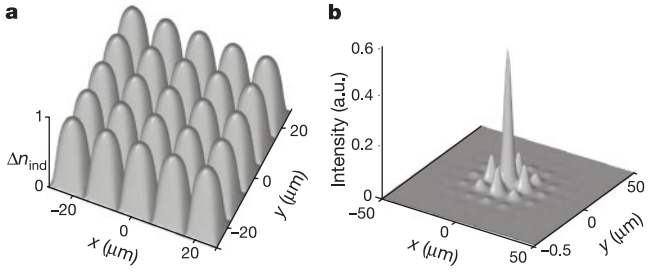

Figure 2 Numerical simulation results depicting the induced photonic lattice and the structure of an on-axis lattice soliton. **a**, Calculated 2D structure of the induced index change (photonic lattice) for the self-focusing nonlinearity. **b**, Simulated intensity structure of the on-axis lattice soliton.

simple creation of photonic lattices in any photosensitive medium of sufficient anisotropy. Theoretically, the dynamical evolution of the system along z is governed by two coupled equations that describe the slowly-varying amplitudes of the lattice wave V (periodic along x and y) and the (soliton-forming) probe U (ref. 12):

$$i\frac{\partial U}{\partial z}+\frac{1}{2k_1}\left(\frac{\partial^2 U}{\partial x^2}+\frac{\partial^2 U}{\partial y^2}\right)-\Delta n_1(I)U=0 \quad (1)$$

$$i\frac{\partial V}{\partial z}+\frac{1}{2k_2}\left(\frac{\partial^2 V}{\partial x^2}+\frac{\partial^2 V}{\partial y^2}\right)-\Delta n_2(I)V=0 \quad (2)$$

Here, the subscripts indicate the orthogonal polarization directions, n_1 and n_2 are the respective indices of refraction, $k_1 = k_0 n_1$, $k_2 = k_0 n_2$, and Δn_1, Δn_2 are the nonlinear index changes induced by the total intensity $I = |U|^2 + |V|^2$. For our specific experiment, $\Delta n_1 = [k_0 n_e^3 r_{33} E_0/2][1+I]^{-1}$ and $\Delta n_2 = [k_0 n_o^3 r_{13} E_0/2][1+I]^{-1}$ are the index changes created by the photorefractive screening nonlinearity[26,27], where the intensity I is measured in units of the background illumination. In these expressions, E_0 is the applied field and $\{n_1 = n_e,\ r_{33}\}$ and $\{n_2 = n_o,\ r_{13}\}$ are the indices of refraction and electro-optic coefficient for the extraordinarily polarized probe beam U and ordinarily polarized array wave V, respectively. We chose a highly anisotropic SBN:75 crystal, in which the nonlinear coefficient $n_o^3 r_{13}$ for V is more than 20 times smaller than the nonlinear coefficient $n_e^3 r_{33}$ for U, implying that Δn_2 is negligible and the dynamics of the array wave is indeed linear. (Note that under suitable conditions, this reduced system of equations can further simplify[12] into a discrete nonlinear Schrödinger equation[2].) An additional assumption in equation (1) is that the photorefractive screening nonlinearity acts isotropically in x and y. This is well justified for our parameters considering that photorefractive screening solitons are almost circular, as are their induced waveguides[28]. The periodic structure of the waveguide array is implicitly contained in the potential induced by $|V(x,y)|^2$. For our representative case of a square lattice of side D formed by four symmetrically interfering plane waves, the lattice intensity $|V|^2 = V_0^2[\cos(\pi x/D) + \cos(\pi y/D)]^2$ provides a periodic potential for the probe field U. In this scenario, the probe (soliton) beam experiences the familiar competition between nearest-neighbour coupling and nonlinearity. We note that the sign of our nonlinearity (whether it is self-focusing or self-defocusing) as well as its magnitude, can be controlled through the polarity and strength of the bias field E_0.

Our experimental set-up is sketched in Fig. 1a. We use a 6-mm-long SBN:75 crystal, with electro-optic coefficients $r_{13} \approx 67\,\mathrm{pm\,V^{-1}}$ and $r_{33} \approx 1,340\,\mathrm{pm\,V^{-1}}$. As a representative geometry, we induce a 2D square photonic lattice (2D array of 2D waveguides) by interfering two pairs of ordinarily polarized plane waves. A typical experimental result (extracted from a 6 mm × 6 mm optically induced photonic lattice) is shown in Fig. 1b, in which each waveguide has a diameter of about 7 μm, with an 11 μm separation between its nearest neighbours. The probe (soliton-forming) beam is extraordinarily polarized and is focused into one of the waveguides, both to maximize the propagation effects through the periodic potential and to yield the narrowest possible lattice solitons. (We note that we are able to generate broader solitons by launching the probe beam into more than one channel and using lower applied fields.) Each array-forming plane wave has 15 mW of power, while the intensity ratio between the entire optical lattice and the probe beam is 5:1. Voltage applied against (along) the c axis sets the focusing (or defocusing) photorefractive screening nonlinearity and, in the proper parameter range, leads to localization of the probe beam and to the formation of lattice solitons. The crystal is also illuminated uniformly (from the top) with a background beam of white light, facilitating fine-tuning of the saturation level of the photorefractive screening nonlinearity.

We first consider on-axis propagation and in-phase lattice solitons. In this regime, the probe beam U experiences normal diffraction, so bright solitons necessitate a self-focusing nonlinearity for which E_0 must be positive. The calculated 2D structure of the induced index change (photonic lattice) and the intensity of the on-axis soliton are shown in Figs 2a and b, respectively. Our experimental results are shown in Fig. 3. Shown is the intensity of the probe beam as it exits the photonic lattice after propagating 6 mm along the 2D waveguide array. This probe beam is launched into a single (the central) waveguide. At low voltages, the probe propagates linearly, and as a result discrete diffraction concentrates the signal intensity into the outer perimeter of a square (Fig. 3a). For a stronger nonlinearity (at a higher voltage), self-focusing dominates and a lattice soliton (a 2D discrete soliton) forms (Fig. 3b). The soliton structure consists of a central intensity peak surrounded by weaker side lobes. An interferogram of this soliton, obtained by interfering the soliton output beam with a plane wave, shows constructive interference of all the elements; that is, the central peak is in-phase with its neighbours (Fig. 3c). As the signal intensity

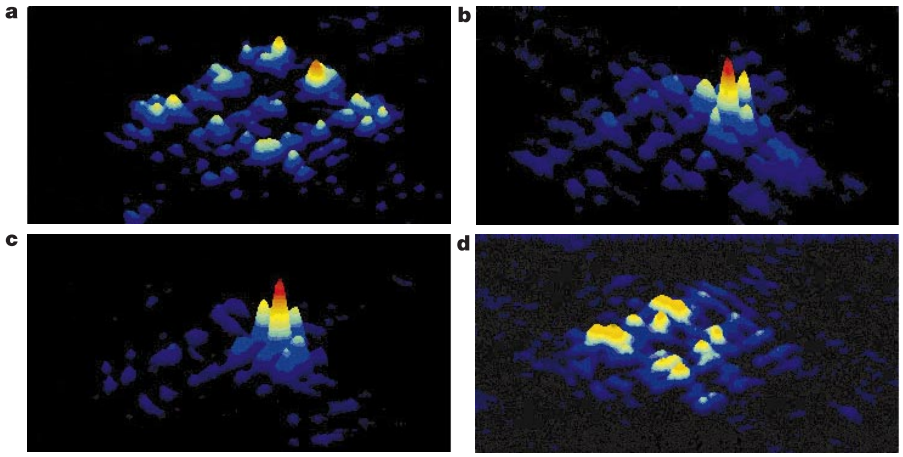

Figure 3 Experimental results presenting the propagation of a probe beam launched into a single waveguide at normal incidence (on-axis propagation). **a**, Intensity structure of the probe beam at the exit face of the crystal, displaying discrete diffraction at low nonlinearity (200 V). **b**, Intensity structure of the probe beam at the exit face of the crystal, displaying an on-axis lattice soliton at high nonlinearity (800 V). **c**, Interferogram, showing constructive interference of peak and lobes between the soliton and a plane wave. **d**, Reduction of probe intensity by a factor of eight, at the same voltage as **b** and **c**, results in recovery of discrete diffraction pattern.

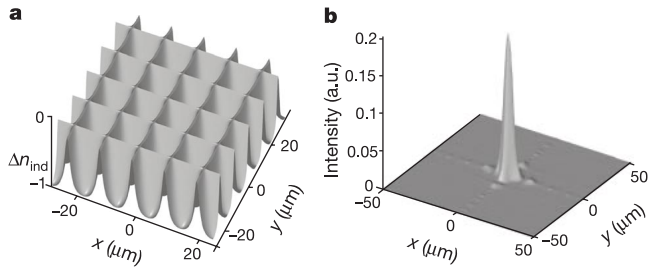

Figure 4 Numerical simulation results depicting the induced photonic lattice and the propagation of a self-trapped staggered wave packet. **a**, Calculated 2D structure of the induced index change (photonic lattice) for the self-defocusing nonlinearity. **b**, Simulated intensity structure of the self-trapped staggered wave packet after 3 cm propagation in our system. As shown here, the energy leakage along the backbone grid is minimal.

is lowered, at the same voltage, the soliton disappears: the beam broadens and the discrete diffraction pattern reappears (Fig. 3d). Because the voltage remains constant, these results imply that the lowered intensity forces the probe beam off the soliton existence curve, that is, the formation of a lattice soliton is an inherently nonlinear effect, which critically depends on the intensity of the soliton beam.

Next, we examine off-axis propagation for which the 'Bloch momentum' of the probe beam lies in the vicinity of the edge of the first Brillouin zone, so that waves propagating in neighbouring waveguides are π out-of-phase with one another. To observe the behaviour, we launch the probe (soliton-forming) beam into a single waveguide of the same array at an angle of 0.55° with respect to the lattice plane. Diffraction in this (angular) region is anomalous (negative)[13]. Hence, self-trapping of a 'bright' wave packet in this regime necessitates a self-defocusing nonlinearity[11,15], that is, E_0 has to be negative. The calculated 2D structure of the induced index change (photonic lattice) is shown in Fig. 4a. Notice that, in contrast to the self-focusing case (of Fig. 2), here adjacent waveguides are not fully isolated from one another but are connected through a grid of narrow equipotential 'backbones', which can allow power to leak slowly along this grid. However, this potential can still support self-trapping of staggered wave packets for a considerable distance, because the energy leakage is very slow. We simulate the propagation of such a self-trapped wave packet, and find it remains a self-trapped entity for very many tunnelling lengths. A typical numerical result is shown in Fig. 4b, which displays the intensity of a self-trapped staggered wave packet after 3 cm propagation in our system. Lines of radiation can be seen along the axes of the array, but their magnitude emphasizes that the power leakage is indeed very small. Our experimental results are shown in Fig. 5. Shown is the intensity of the probe beam as it exits the photonic lattice after propagating 6 mm along the 2D waveguide array. At low voltages, a diffuse diffraction pattern occurs (Fig. 5a), while a staggered (π out-of-phase) self-trapped wave packet is observed (Fig. 5b) at a higher nonlinearity. Indeed, an interferogram (Fig. 5c) confirms this staggered interpretation: the central peak is lowered while the surrounding lobes increase their intensity, indicating destructive and constructive interference, respectively. When the intensity of the probe is lowered, while keeping the voltage across the crystal constant, the diffuse diffraction pattern is recovered (Fig. 5d).

We emphasize that under the same experimental conditions, without the presence of the periodic lattice, no soliton formation is observed. This effect is very pronounced in the staggered case (Fig. 5), where removing the periodic lattice while keeping the negative voltage (self-defocusing nonlinearity) leads to increased expansion of the probe beam, much beyond its natural (linear) diffraction. In the on-axis case (Fig. 3), removing the periodic lattice while keeping the positive voltage shows some small self-focusing of the probe beam, but the ratio between the probe and background beam intensities is off the soliton existence curve and cannot support a soliton[26–28]. Hence, the soliton formation results presented in Figs 3 and 5, under their experimental conditions, correspond solely to lattice solitons.

The photonic lattice is optically induced by interfering pairs of plane waves in a photosensitive (photorefractive) material, giving our system the exciting capability of fully controlling and reversing both diffraction and nonlinearity. This can be achieved only in dynamical systems such as photorefractive crystals or possibly nematic liquid crystals (for optical waves) or in Bose–Einstein condensates (for matter waves). The technique of optical induction allows for reconfigurable arrays of almost any geometry or Bravais symmetry, including defect states and various three-dimensional

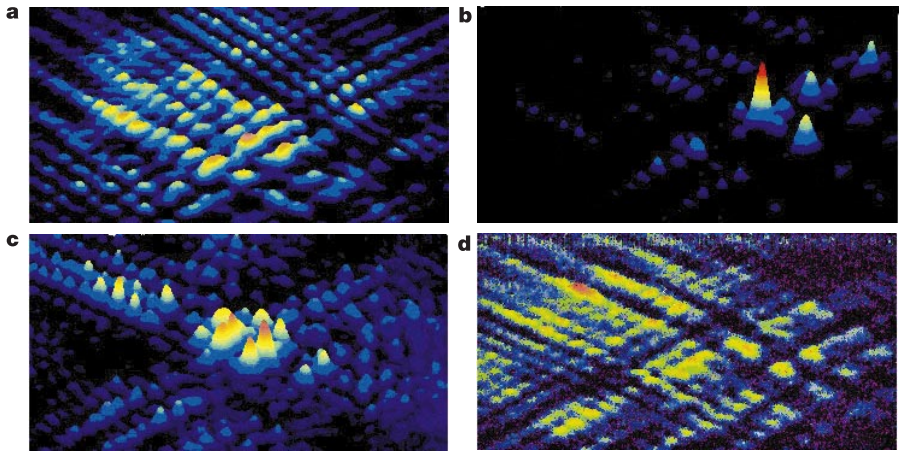

Figure 5 Experimental results presenting the propagation of a probe beam launched into a single waveguide. The angle of the beam is 0.55° with respect to the lattice plane, corresponding to the edge of the first Brillouin zone. **a**, Intensity structure of the probe beam at the exit face of the crystal, displaying diffuse diffraction at low nonlinearity (−200 V). **b**, Intensity structure of the probe beam at the exit face of the crystal, displaying a self-trapped staggered wave packet at high nonlinearity (−800 V). **c**, Interferogram, showing destructive interference of peak and constructive interference of lobes, between the self-trapped wave packet and a plane wave. **d**, Reduction of probe intensity by a factor of eight, at the same voltage as **b** and **c**, results in recovery of diffuse diffraction pattern.

structures. Our results pave the way for the realization of a variety of nonlinear localization phenomena in photonic lattices and crystals[19–23]. Given the potential of photonic structures for miniaturized optical devices[29], we anticipate that lattice solitons, being highly nonlinear entities controlled by light alone[30], will become of increasing importance. Finally, our observation directly relates to the proposed lattice solitons in Bose–Einstein condensates[4], which can be observed in optically induced periodic potentials[24,25]. □

Received 26 September 2002; accepted 21 January 2003; doi:10.1038/nature01452.

1. Davydov, A. S. & Kislukha, N. I. Solitary excitations in one-dimensional molecular chains. *Phys. Status Solidi B* **59,** 465–470 (1973).
2. Christodoulides, D. N. & Joseph, R. I. Discrete self-focusing in nonlinear arrays of coupled waveguides. *Opt. Lett.* **13,** 794–796 (1988).
3. Su, W. P., Schieffer, J. R. & Heeger, A. J. Solitons in polyacetylene. *Phys. Rev. Lett.* **42,** 1968–1971 (1979).
4. Trombettoni, A. & Smerzi, A. Discrete solitons and breathers with dilute Bose-Einstein condensates. *Phys. Rev. Lett.* **86,** 2353–2356 (2001).
5. Xie, A., van der Meer, L., Hoff, W. & Austin, R. H. Long-lived amide I vibrational modes in myoglobin. *Phys. Rev. Lett.* **84,** 5435–5438 (2000).
6. Trias, E., Mazo, J. J. & Orlando, T. P. Discrete breathers in nonlinear lattices: experimental detection in Josephson junctions. *Phys. Rev. Lett.* **84,** 741–744 (2000).
7. Schwartz, U. T., English, L. Q. & Sievers, A. J. Experimental generation and observation of intrinsic localized spin wave modes in an antiferromagnet. *Phys. Rev. Lett.* **83,** 223–226 (1999).
8. Swanson, B. I. *et al.* Observation of intrinsically localized modes in a discrete low-dimensional material. *Phys. Rev. Lett.* **82,** 3288–3301 (1999).
9. Eisenberg, H. S., Silberberg, Y., Morandotti, R., Boyd, A. R. & Aitchinson, J. S. Discrete spatial optical solitons in waveguide arrays. *Phys. Rev. Lett.* **81,** 3383–3386 (1998).
10. Morandotti, R., Eisenberg, H. S., Silberberg, Y., Sorel, M. & Aitchison, J. S. Self-focusing and defocusing in waveguide arrays. *Phys. Rev. Lett.* **86,** 3296–3299 (2000).
11. Fleischer, J. W., Carmon, T., Segev, M., Efremidis, N. K. & Christodoulides, D. N. Observation of discrete solitons in optically-induced real-time waveguide arrays. *Phys. Rev. Lett.* **90,** 023902 (2003).
12. Efremidis, N. K., Sears, S., Christodoulides, D. N., Fleischer, J. W. & Segev, M. Discrete solitons in photorefractive optically-induced photonic lattices. *Phys. Rev. E* **66,** 046602 (2002).
13. Eisenberg, H., Silberberg, Y., Morandotti, R. & Aitchison, J. Diffraction management. *Phys. Rev. Lett.* **85,** 1863–1866 (2000).
14. Ablowitz, M. J. & Musslimani, Z. H. Discrete diffraction-managed spatial solitons. *Phys. Rev. Lett.* **87,** 254102 (2001).
15. Kivshar, Y. S. Self-localization in arrays of defocusing waveguides. *Opt. Lett.* **18,** 1147–1149 (1993).
16. Scott, A. C. & Macneil, L. Binding energy versus nonlinearity for a "small" stationary soliton. *Phys. Lett. A* **98,** 87–88 (1983).
17. Lederer, F., Darmanyan, S. & Kobyakov, A. in *Spatial Solitons* (eds Trillo, S. & Torruellas, W.) 269–292 (Springer, New York, 2001).
18. Malomed, B. A. & Keverkidis, P. G. Discrete vortex solitons. *Phys. Rev. E* **64,** 026601 (2001).
19. Chen, W. & Mills, D. L. Gap solitons and the nonlinear optical response of superlattices. *Phys. Rev. Lett.* **58,** 160–163 (1987).
20. Christodoulides, D. N. & Joseph, R. I. Slow Bragg solitons in nonlinear periodic structures. *Phys. Rev. Lett.* **62,** 1746–1749 (1989).
21. John, S. & Akozbek, N. Nonlinear optical solitary waves in a photonic band gap. *Phys. Rev. Lett.* **71,** 1168–1171 (1993).
22. Mingaleev, S. F. & Kivshar, Y. S. Self-trapping and stable localized modes in nonlinear photonic crystals. *Phys. Rev. Lett.* **86,** 5474–5477 (2001).
23. Christodoulides, D. N. & Efremidis, N. K. Discrete temporal solitons along a chain of nonlinear coupled microcavities embedded in photonic crystals. *Opt. Lett.* **27,** 568–570 (2002).
24. Anderson, B. P. & Kasevich, M. A. Macroscopic quantum interference from atomic tunnel arrays. *Science* **282,** 1686–1689 (1998).
25. Greiner, M., Mandel, O., Hänsch, T. W. & Bloch, I. Collapse and revival of the matter wave field of a Bose–Einstein condensate. *Nature* **419,** 51–54 (2002).
26. Segev, M., Crosignani, B., DiPorto, P., Valley, G. C. & Yariv, A. Steady state spatial screening-solitons in photorefractive media with external applied field. *Phys. Rev. Lett.* **73,** 3211–3214 (1994).
27. Christodoulides, D. N. & Carvalho, M. I. Bright, dark, and gray spatial soliton states in photorefractive media. *J. Opt. Soc. Am. B* **12,** 1628–1633 (1995).
28. Shih, M., Segev, M. & Salamo, G. Circular waveguides induced by two-dimensional bright steady-state photorefractive spatial screening solitons. *Opt. Lett.* **21,** 931–933 (1995).
29. Joannopoulos, J. D., Meade, R. D. & Winn, J. N. *Photonic Crystals: Molding the Flow of Light* (Princeton Univ. Press, Princeton, New Jersey, 1995).
30. Christodoulides, D. N. & Eugenieva, E. D. Blocking and routing discrete solitons in two-dimensional networks of nonlinear waveguide arrays. *Phys. Rev. Lett.* **87,** 233901 (2001).

Acknowledgements This work is part of the MURI programme on optical solitons, and was also supported by the Israeli Science Foundation, and by the German–Israeli DIP project. J.W.F thanks the Lady Davis Foundation at the Technion for support.

Competing interests statement The authors declare that they have no competing financial interests.

Correspondence and requests for materials should be addressed to M.S. (e-mail: msegev@tx.technion.ac.il).

Self-organization of dissolved organic matter to micelle-like microparticles in river water

Martin Kerner*†, Heinz Hohenberg‡, Siegmund Ertl§, Marcus Reckermann‖ & Alejandro Spitzy§

** University of Hamburg, Institute for Hydrobiology and Fishery Science, D-22765 Hamburg, Zeiseweg 9, Germany*
‡ Heinrich-Pette-Institute for Experimental Virology and Immunology, University of Hamburg, Martinistr. 52, D-20251 Hamburg, Germany
§ University of Hamburg, Institute for Biogeochemistry and Marine Chemistry, D-20146, Hamburg, Bundesstrasse 55, Germany
‖ Research and Technology Centre Westcoast, University of Kiel, D-25761 Büsum, Hafentörn, Germany

In aquatic systems, the concept of the 'microbial loop' is invoked to describe the conversion of dissolved organic matter to particulate organic matter by bacteria[1]. This process mediates the transfer of energy and matter from dissolved organic matter to higher trophic levels, and therefore controls (together with primary production) the productivity of aquatic systems. Here we report experiments on laboratory incubations of sterile filtered river water in which we find that up to 25% of the dissolved organic carbon (DOC) aggregates abiotically to particles of diameter 0.4–0.8 micrometres, at rates similar to bacterial growth. Diffusion drives aggregation of low- to high-molecular-mass DOC and further to larger micelle-like microparticles. The chemical composition of these microparticles suggests their potential use as food by planktonic bacterivores. This pathway is apparent from differences in the stable carbon isotope compositions of picoplankton and the microparticles. A large fraction of dissolved organic matter might therefore be channelled through microparticles directly to higher trophic levels—bypassing the microbial loop—suggesting that current concepts of carbon conversion in aquatic systems require revision.

We studied the capacity for abiotic aggregation of dissolved organic matter (DOM) less than 0.2 μm in diameter present in sterile filtered Elbe water, sampled from the surface at the study site at kilometre 627 (53.543335° N, 9.914018° E) during summer and autumn (June and November 2000) and preserved with 0.02% (w/v) NaN_3, in 5-litre batch experiments under mild agitation in the dark. These experimental procedures ensured diffusion (brownian motion) providing the necessary energy[2] for aggregation of exclusively natural DOM in the absence of bacteria[3] whose numbers remained undetectable below 100 cells ml^{-1} throughout the experiments by transmission electron microscopy (TEM)[4]. Heterotrophic processes were effectively suppressed, because total organic carbon remained constant. Over the experimental period of ten days, abiotic microparticle formation at 24 °C was found to consume about 25% and 7% of the total initial dissolved organic carbon present at similar concentrations in summer and autumn, respectively (Fig. 1a, b). Production rates and abundances of microparticles reached those of bacteria in the river Elbe and in many other rivers and estuaries[5] (Table 1). Significant amounts of DOC in these environments might therefore be transformed into microparticulate matter by aggregation and not by heterotrophic processes, as is currently assumed.

Flow cytometry revealed that the diameters of the microparticles remain within a narrow range between 0.4 and 0.8 μm. Formation within this restricted size range contrasts the assembly of polymer gels of up to 5 μm described for ocean water under non-turbulent

† Present address: SSC Strategic Science Consult Ltd, D-22765 Hamburg, Bodenstedtstr. 16, Germany.

